Assembly Gap Variation Methods for the Westinghouse ANC Nodal Code

David C. Little and Robert J. Fetterman
Westinghouse Electric Company
P.O. Box 355
Pittsburgh, PA 15230
The United States of America
littledc/fetterrj@westinghouse.com

Abstract

Standard design methods and modeling practice for node configurations in the Westinghouse Advanced Nodal Code (ANC) assume nominal assembly pitch and interstitial assembly gaps. Modeling variable assembly gaps and pitch in ANC require adjustments to both the nodal solution and pin power reconstruction for the localized lattice effects along the outer assembly node boundaries. These effects must account for the immediate spatial effects for water variations along the node boundaries and the diagonal node gap configuration, as well as the accumulated historical effects with burnup. Ignoring these effects can lead to pin power differences as much as 20 percent compared with higher order methods. When accounting for all of the nodal and lattice effects, the pin powers were shown to give similar accuracy to the nominal modeling results.

Introduction

Average, interstitial-assembly, grid-to-grid gaps, as modeled in standard design calculations, are typically ~2 millimeters. The fuel support plates constrain the assembly gaps at the top and bottom of the fuel assembly to near nominal sizes, however the core mid-plane can have larger gap variations. In theory, the largest gap could be nearly 30 millimeters, though this is highly unlikely. However, in-core, mid-plane gap sizes of 5-6 times the nominal gap size are possible per calculations from a code called SAVAN. Per the 3D gap predictions by SAVAN, the largest gaps are anticipated to occur infrequently in the core interior, where the impact on power peaks is likely to be more significant.

The changes in methodology required to model the reactivity and power impacts due to gap variations in a nodal code is the subject of this study. Proper neutronics modeling of these variations in the 3D context requires that the local lattice effects be captured in a full core, 3D model. Existing neutronics codes which can model full 3D cores can not practically account for the explicit, pin-wise lattice variations which result from non-uniform assembly pitches radially about the core.

The Westinghouse Advanced Nodal Code[1] (ANC) is a 3-dimensional nodal code, which uses macroscopic depletion with certain explicit microscopic feedbacks and

homogeneous-to-heterogeneous corrections. There are typically four nodes per assembly radially, where all have the same node pitch, and thus the same gap, in the x- and y-directions. Only, the axial node mesh sizes are variable. The nodal solution of ANC uses the Nodal Expansion Method (NEM) to solve the coupled 1D diffusion equation for each of the x, y, and z coordinates. The nodal balance and coupling equations are derived in terms of interface net currents. Per time step, one set of discontinuity factors per node is used to correct the currents for heterogeneous effects not represented by the homogeneous cross-sections. For standard PWR design practice, one set is sufficient for all four faces of the node, since the two internal assembly faces of adjacent nodes should cancel in their effects, and the two external assembly faces are nearly the same for standard fuel design products.

After the global solution is obtained, the intranodal pin power distribution is recovered for every node using an efficient superposition procedure. Using the surface flux of the nodes from the NEM solution as boundary conditions, the homogeneous power distribution is obtained from the homogeneous flux multiplied by node average kappa-fission cross-section, where g is the fast and thermal energy groups:

$$P_{g,homo}(x,y) = \phi_{g,homo}(x,y)\ \kappa\Sigma_{fg} \qquad (1)$$

$P_{g,homo}(x,y)$ is then adjusted for the intranodal burnup gradient, using the relative $\kappa\Sigma_{fg}(x,y)$ distribution constructed from the node surface burnups. Finally, the pin-wise heterogeneous distribution is obtained by multiplying by a group-dependent pin factor. A pin factor is the ratio of the heterogeneous-to-homogeneous pin power by neutron energy group from a reference PHOENIX-P^2 unit assembly (UA) calculation, where the homogeneous flux is constant due to reflective symmetry. Therefore:

$$P_{g,hetero}(x,y) = \phi_{g,homo}(x,y)\ \kappa\Sigma_{fg}(x,y)\ PF_g(x,y) \qquad (2)$$

where $PF_g(x,y) = P_{g,hetero}(x,y) / P_{g,homo}(x,y)$ from the UA
Note: $P_{g,homo}(x,y)$ is constant for all x,y of the UA node

Discussion of Method Changes

The variation in assembly gaps across the core, require many adjustments and additions to the methods described above. These gaps can range from no gap (grid-to-grid closure) to many times the nominal gap size represented by the ANC node. The following is a list of the major additions/changes to the methods:

General additions:

1. Obtain/define the two external gaps per each node;
2. Generate gap-specific cross-section, discontinuity factor, and pin factor data using PHOENIX-P UAs over the anticipated range of gap sizes;

Nodal solution adjustments per node:

3. Volume correct macroscopic cross-sections for use in ANC node based on nominal gap size;
4. Set up gap-dependent table of discontinuity factors, which are those for the nominal gap, adjusted for gap-specific spectral change and burnup trends (see discussion below);
5. Look up (via interpolation) cross-sections and discontinuity factors based on each node's average gap and burnup;
6. Using integrated spectrum with burnup due to gap history, lookup the corrections to the node's macroscopic cross-sections due to differences in isotopics (mainly actinides) from the UA which generated them;

Pin power reconstruction per node:

7. Lookup pin factors ($PF_g(x,y)$) for both gaps of the node;
8. Correct the two gap-specific sets of pin factors for differences in the actual node pin-wise burnup versus the pin-wise burnup found in the UAs;
9. Blend the two sets of gap-specific pin factors into one effective set for the node with two gaps;
10. Correct edge pin factors for edge pin fissile burnout due to local spectral history differences; and
11. Correct the blended set of pin factors for the actual versus implied gap configuration at the assembly corner, including the integrated delta burnup effects. Note that the actual corners of assemblies are dependent on the accumulated gaps along the assembly rows and columns.

Nodal solution issues:

For the ANC nodal solution, the cross-section treatments, such as volume correction and interpolation based on node-average gap, are performed as would be expected. Only the approximations to the discontinuity factors (item 4) to obtain one set per node and the effects with burnup on cross-sections (item 6) due to explicit gap history from cycle to cycle require further explanation.

Gap variations would suggest face-dependent discontinuity factors should be applied, however, ANC only accepts one set for all four faces of a node. A method was derived to calculate one set per node and preserve node average power accuracy with gap variation. Since neighbor assemblies share the same gaps, changes to the gap will have about the same effect on the fluxes near the surfaces of both assemblies. There should be little change to the fluxes on the internal assembly node interfaces due to gap. Thus, the leakage conditions for the variable gaps should be similar to the nominal gap configurations, suggesting that use of the nominal discontinuity factors could be applied. However, to obtain the nominal gap flux spectrum at the node surface requires a correction due to the node average flux spectrum which includes the variable gap effects.

The flux spectrum of variable versus nominal gap for a node can be approximated by dividing the thermal absorption (Σ_{a2}) by the removal (Σ_r) macroscopic cross-sections for each of the two conditions. This correction need only apply to the thermal discontinuity factors, since the fast flux will change at about the same rate that the power changes. The gap impact is predominantly a thermal flux effect.

One residual effect of the gaps is the trend with burnup which must be applied to the fast, as well. Therefore, to account for the spectral and burnup effects on the discontinuity factors and return the surface fluxes to near nominal conditions, the following discontinuity factor calculations are made:

$$DF1_{gap,bu} = DF1_{nomgap,BOC} \times \frac{DF1_{gap,bu}}{DF1_{gap,BOC}} \tag{3}$$

$$DF2_{gap,bu} = DF2_{nomgap,BOC} \times \frac{DF2_{gap,bu}}{DF2_{gap,BOC}} \times \frac{\left(\frac{\Sigma_{a2}}{\Sigma_r}\right)_{gap}}{\left(\frac{\Sigma_{a2}}{\Sigma_r}\right)_{nomgap}} \tag{4}$$

The gap-dependent cross-section table takes into account the effects of burnup with variable gaps within a cycle, provided a node's gap sizes due not change appreciably during the cycle. With multiple cycles, however, the gaps can vary dramatically and too many gap scenarios exist to include in the table. The PHOENIX-P UAs for burned fuel are generated assuming nominal gap depletion up to the current cycle burnups, as demonstrated in Figure 1. A method is needed to adjust the macroscopic cross-sections per node for prior cycle history effects, mainly due to actinide differences.

Based on a study of several gap scenarios over several cycles using PHOENIX-P UA models, the following observations were made:

1. The percent correction to the cross-sections at the beginning-of-cycle (BOC) versus the ratio of the cumulative, actual-to-nominal gap, spectra, integrated with respect to burnup yields a family of linear curves based on node burnup and current gap size, as illustrated in Figure 2, and
2. During the current cycle the correction can be decayed away using an exponential relationship, as illustrated in Figure 3.

Pin Power Reconstruction Issues:

Unlike the cross-sections, the pin factors must explicitly account for both gaps of the node. This involves a blending process (item 9) of the pin factors from the UAs, generated for both of the gaps. This process is designed to preserve the relative pin factor shape of the rows and columns from one or the other of the UAs, depending on the pin and gap locations.

As discussed above, the cross-sections and pin factors for burned fuel are generated from PHOENIX-P UA depletions with nominal gap histories for prior cycles. There are two parts to this correction. One correction (item 8) accounts for the delta pin-wise burnup, or $\kappa\Sigma_f$, distribution of the UAs for the actual two-gap history versus each UA one-gap history. The other correction (item 10) accounts for the local fissile isotopic burnout along the edge pins next to the gap relative to the internal pins, which are not captured by the prior cycle nominal gap history of the UAs.

One final, but significant, correction (item 11) accounts for the implied gap pattern at the assembly corner due to the blending process versus the actual gap configuration, including the diagonally opposite assembly. The blending process assumes reflection of the two gaps of the node to the neighbor nodes, where as the actual locations of neighbor assembly corners is based on the accumulation of the gaps along the assembly rows and columns of the core. This is illustrated in Figure 5. This correction can be quite large (up to 20% in corner pin power) in certain situations. The difference in the implied gap configuration versus the actual gap configuration at the corner of an assembly can either add or subtract water, affecting the amount of moderation, and thus thermal flux seen by the corner of the assembly. The pin factors must account for this over the entire node, requiring the corner pin effect to be decayed into the node.

Qualification/Validation of Methods

Qualification of the ANC method changes and additions made to permit modeling of variable assembly gap was performed by benchmarking ANC models to lattice calculations based on PHOENIX-P and MCNP. PHOENIX-P and MCNP have the ability to explicitly model the pins and gaps of the assemblies Two basic types of models are generated; 1) a PHOENIX-P unit assembly with variation in gaps around the assembly, as illustrated in Figure 5, and 2) a 3x3 assembly mini-core PHOENIX-P and MCNP models with variations in gap, as illustrated in Figures 6 and 7, respectively..

Unit Assembly Model:

The unit assembly (UA) model shown in Figure 5 was depleted with gaps 1,2 3 and 4 varied as follows:

1. First cycle, 0 to 10 GWD/T, with gaps of 4, 12, 0, and 0 mm,
2. Second cycle, 10 to 20 GWD/T, with gaps of 8, 0, 0, and 0 mm,
3. Third cycle, 20 to 28 GWD/T, with gaps of 0, 16, 0, 0 mm,
4. Fourth cycle, 28 to 40 GWD/T, with gaps of 12, 8, 0, and 0 mm, and
5. Fifth cycle, 40 to 60 GWD/T, with gaps of 0, 0, 16 and 16 mm.

This simulates an unlikely, severe gap history effect as an assembly is shuffled to different core locations from cycle to cycle. This model is a very conservative test for the ANC methodology and qualifies all of the new methods except the discontinuity factors,

as applied to the external assembly interfaces, and the corner assembly pin factor correction.

Figures 8 shows the accuracy of the node powers over five cycles with very extreme shifts in gap size for each node. All node power comparisons to PHOENIX-P are mostly within 0.5% and completely within +/- 1% over the first four cycles up to a burnup of 40,000 MWD/MTU. These results are comparable to those found in standard design. The beginning-of-cycle (BOC) of cycle 5 shows two diagonally opposite nodes with the most severe gap shifts, which still give an accuracy of +1.8 % and –1.2%.

The pin power agreement is also generally within +/- 5% throughout the five cycles, when the node differences are removed. Until BOC of Cycle 4 only one edge pin was greater than 1.5%. Figures 9 and 10 show the larger differences at 40,000 MWD/MTU for the end-of-cycle (EOC) for cycle 4 and BOC cycle 5. The few edge pins which show greater than 3% are along the edge are very unlikely to occur due to the severe gap shift modeled. It is also important to note assemblies at these burnups have lower overall power, and the deviations are predicted to be conservatively higher by ANC.

3x3 Assembly Mini-Core Models:

The 3x3 assembly PHOENIX-P mini-core model, shown in Figure 6, can be used as a benchmark for nodal and pin power reconstruction methods, including corner pin factor correction due to corner gap configuration, for conditions at BOL and over one cycle of depletion. Four L1-L2 gap configurations are modeled; 15.5-15.5, 11-8, 8-8 and 8-4 mm gaps. The 15.5 mm gaps are unlikely to occur. Gap sizes of 8 and 11 mm are more likely, but infrequent in the core interior. The MCNP model in Figure 7 illustrates an unlikely concentration of large gaps in the core interior. MCNP allows the offset assembly configuration which can result from gap variations to be modeled explicitly.

The node power comparisons from the 3x3 mini-core models, shown in Figures 11 and 12, show most nodes to be within +/- 1%. The largest difference was –2% for an unlikely gap size. This represents only a slight degradation of accuracy is only slightly relative to standard design.

The pin power comparisons from each of these models contain over 1800 fuel pins, where approximately 97-8% of the pins are within +/-1% with the largest deviations mostly within 2.5%. Figures 13 shows the largest general scatter in the data, partly because MCNP is a Monte Carlo code with statistical variations. Even still, it is well within the anticipated scatter for standard design. Figure 14 shows the largest deviations of the 3x3 model results for a gap size (15.5 mm) which is unlikely and after 20 GWD/MTU in cycle depletion. With exception of the one corner pin at 4.5% deviation, these pins were within +/- 2.5% and generally within +/-1%, which is similar to standard design deviations.

Conclusions and Impact on Actual Core Evaluations

Except for the very largest deviations in this study, the vast majority of node and pin powers are similar to the accuracy observed for nominal ANC versus PHOENIX-P calculations. The deviations from the PHOENIX-P benchmark results which are greater than 2.5% occurred on, or next to, the assembly corners are for situations which are not likely to occur. Realistic gap sizes would reduce the deviations in accuracy to nominal levels. The larger deviations in this study which occur due to gap history at high burnups will generally not be limiting and are generally conservative.

Due to the complexities of modeling burned fuel via input to PHOENIX-P and MCNP, all assemblies were modeled initially as fresh fuel. This flattened the homogeneous solution among the neighbor assemblies, causing the heterogeneous effects to increase the corner and edge pin next to the large gaps. Since fresh fuel assemblies will likely be straight, near nominal gaps are expected between them. Results of the subsequent study using ANC full core models, as applied to a realistic core environment, show that the peak pin power locations do not occur on the edge when burned assemblies are next to fresh assemblies. Only the most burned assemblies are likely to cause large gaps, but also cause the peak pins locations in the neighbor fresh assemblies to move to the assembly interior. For pins even one row in from the edge, the accuracy of these methods is significantly better and the pin power deviations relative to nominal gaps are less than observed in the 3x3 models.

Overall, the methods derived in this study for nodal codes like ANC with pin power reconstruction, give the expected accuracy relative to higher order methods of lattice codes such as PHOENIX-P and MCNP. These methods provide a reliable means to evaluate the impact on nuclear core parameters with gap variation throughout the core.

Acknowledgement

The authors would like to acknowledge the consultation and verification support given by both Y.A. Chao and Larry T. Mayhue, the software support given by Robert W. Flammang, and the MCNP modeling support by Michael J. Hone of the Westinghouse Electric Company for this study.

References

1 Liu, Y.S. et.al., “ANC: A Westinghouse Advanced Nodal Computer Code,” WCAP-10965-A, December 1985.

2 Nguyen, T.Q., et. al., “Qualification of the PHOENIX/ANC Nuclear Design System for Pressurized Water Reactor Cores,” WCAP-11596-A, June 1988.

Figure 1

Illustration of Gap History for a Fuel Node

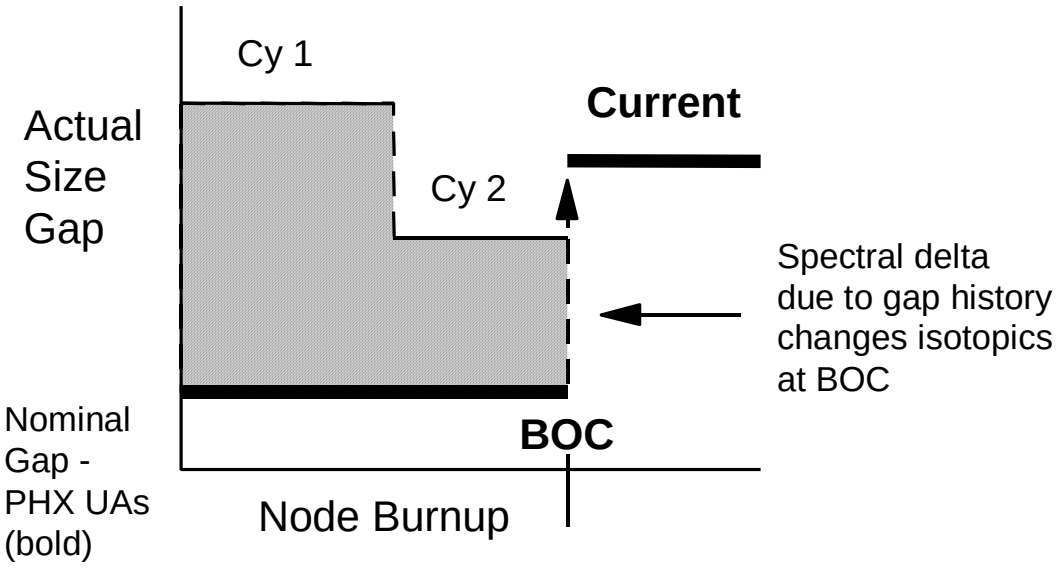

Figure 2

Depletion Effect of Gap History Correction per Cross-section

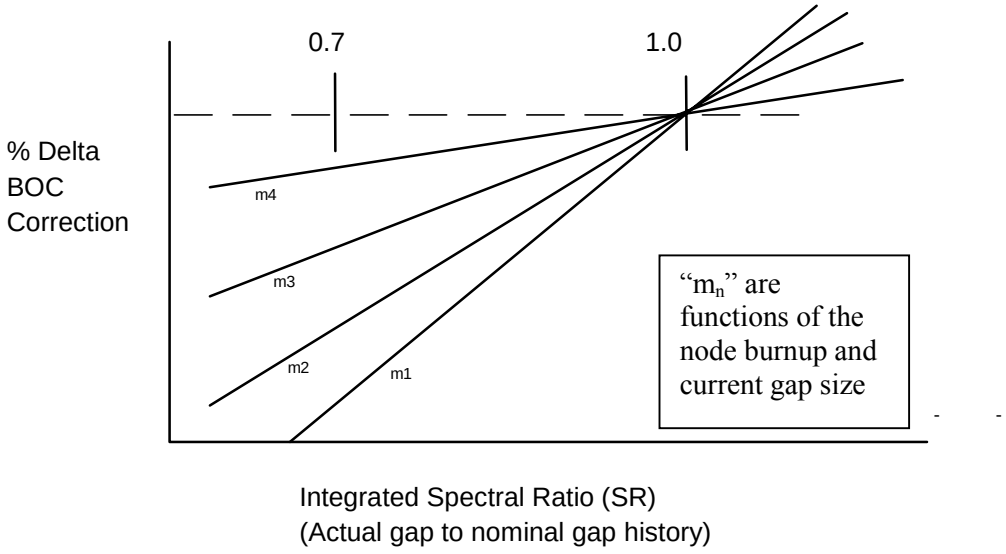

Figure 3

Gap History Correction Process

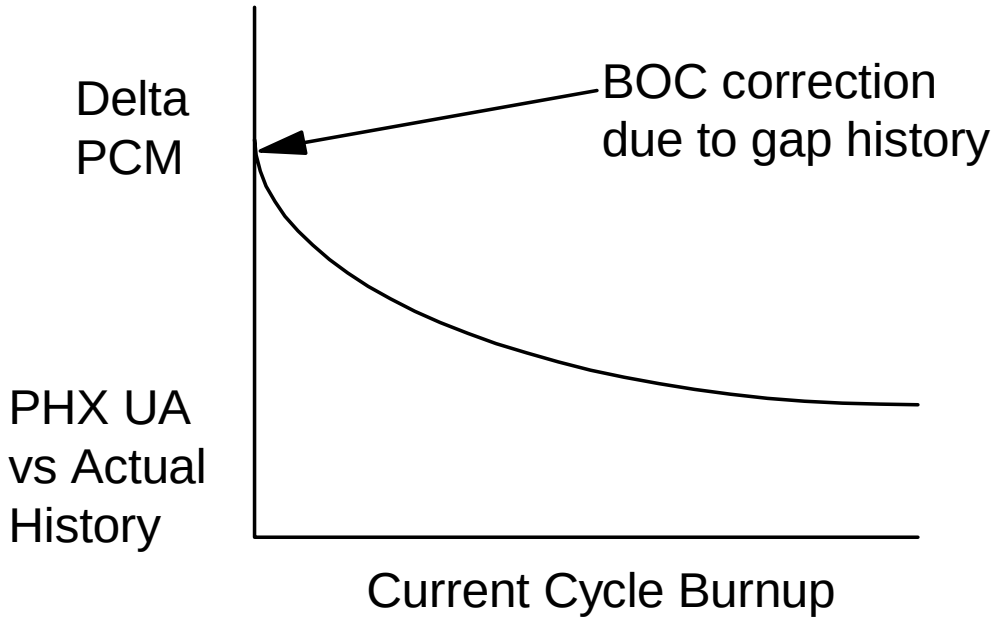

Figure 4

Implied vs Actual Water Volume

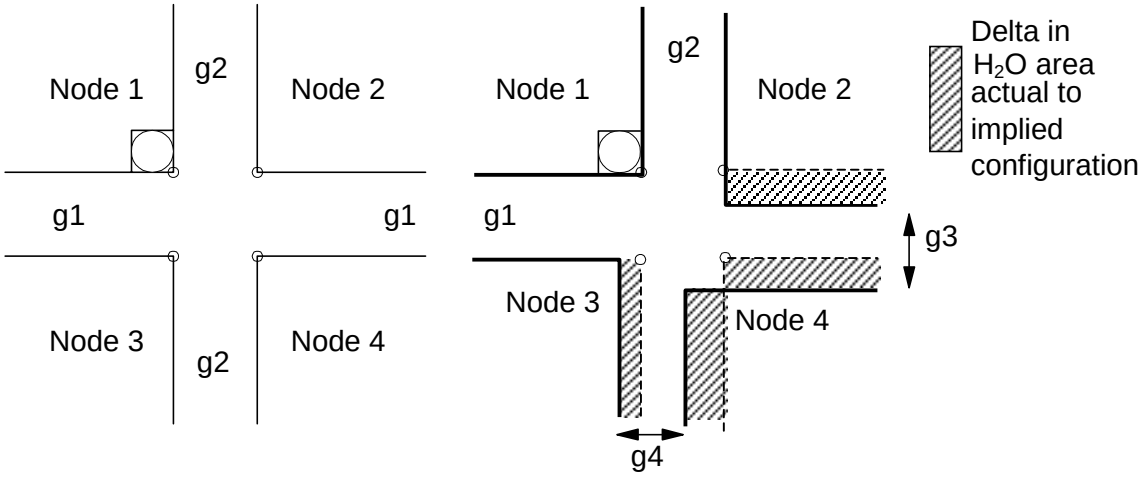

Figure 5
Unit Assembly Model with Gap Variations

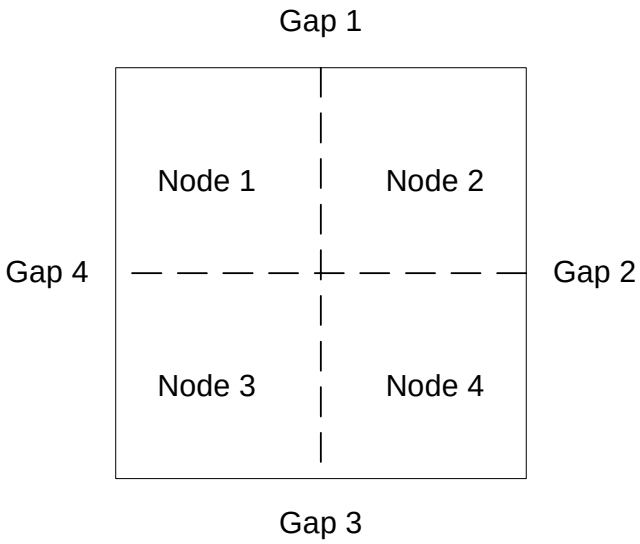

Figure 6
3x3 Assembly Model - Center Gap Variation

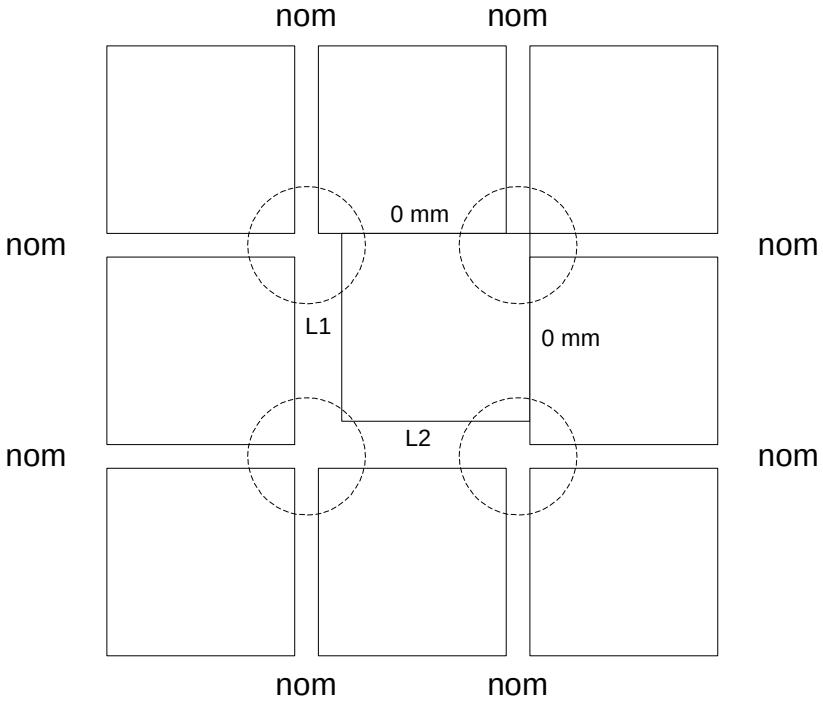

Figure 7

ANC vs MCNP 3x3 Assembly Mini-Core Model

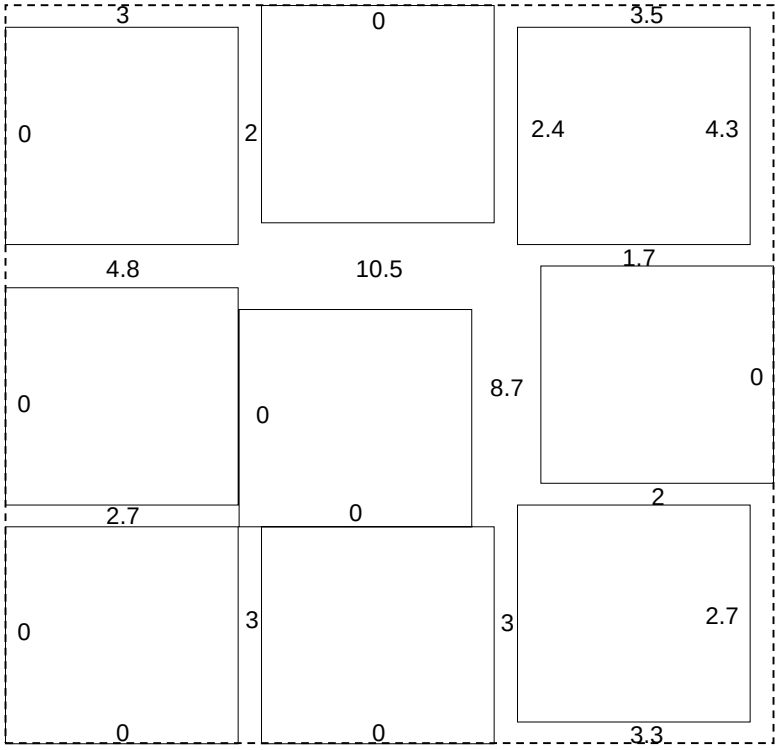

Figure 8

UA Node Power Accuracy with Gap History over Five Cycles

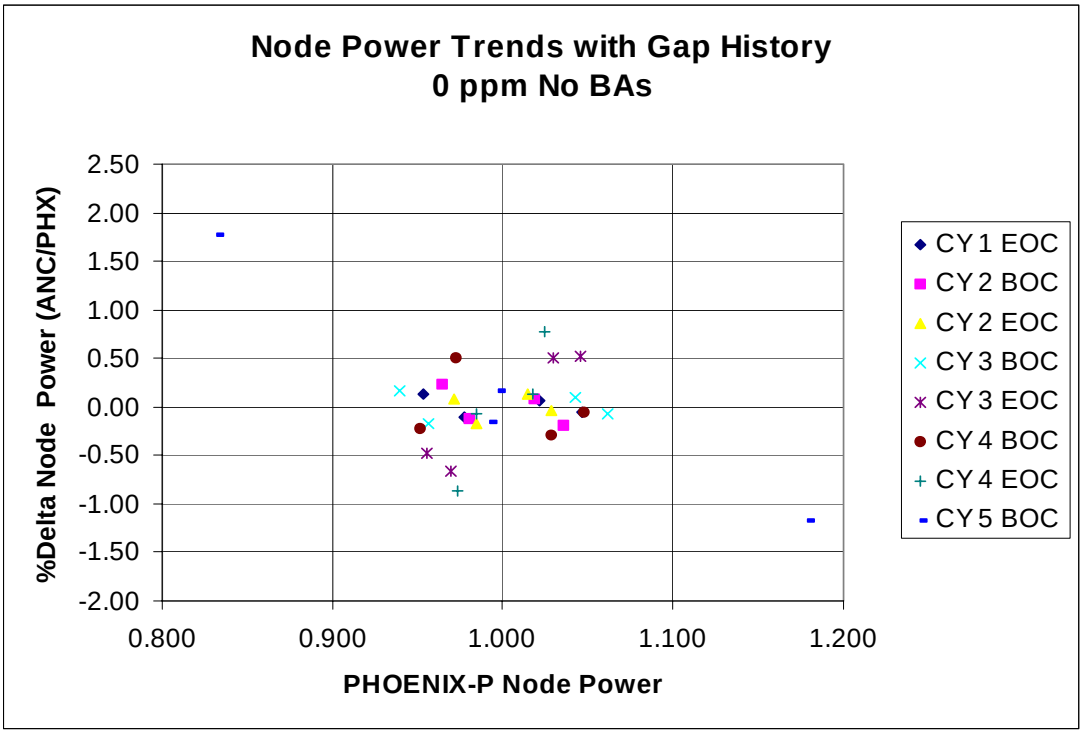

Figure 9
UA Pin Power Accuracy with Gap History EOC Cycle 4

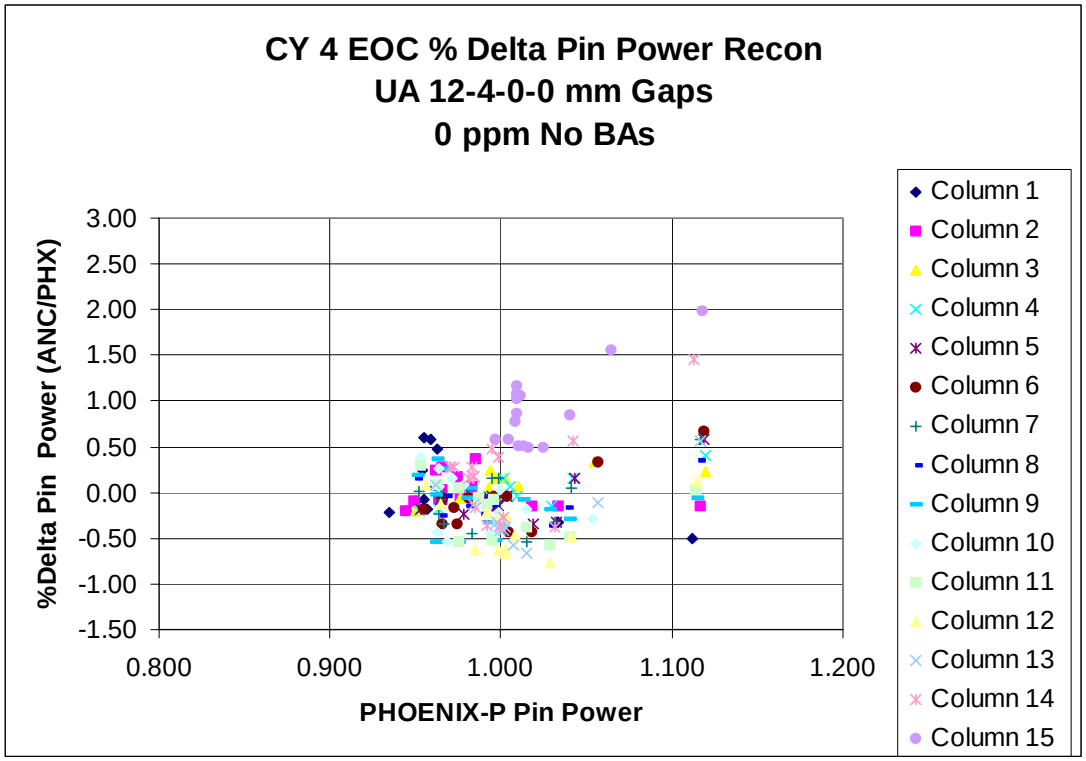

Figure 10
UA Pin Power Accuracy with Gap History BOC Cycle 5

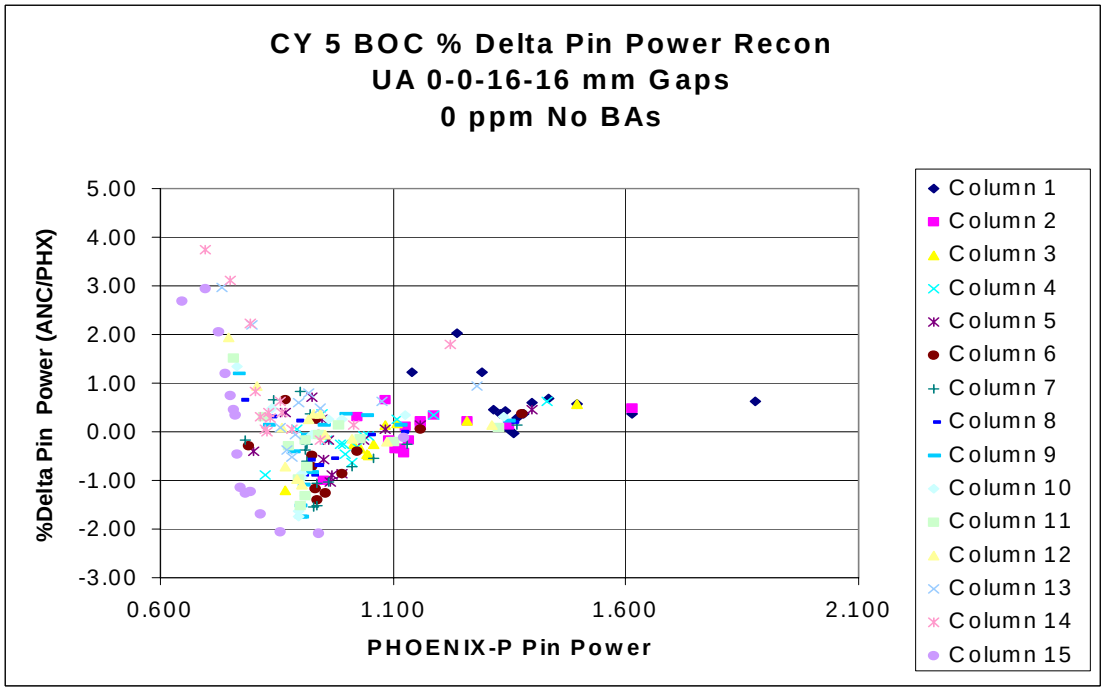

Figure 11
3x3 Model with 15.5 mm Gaps - Node Power Accuracy with Burnup

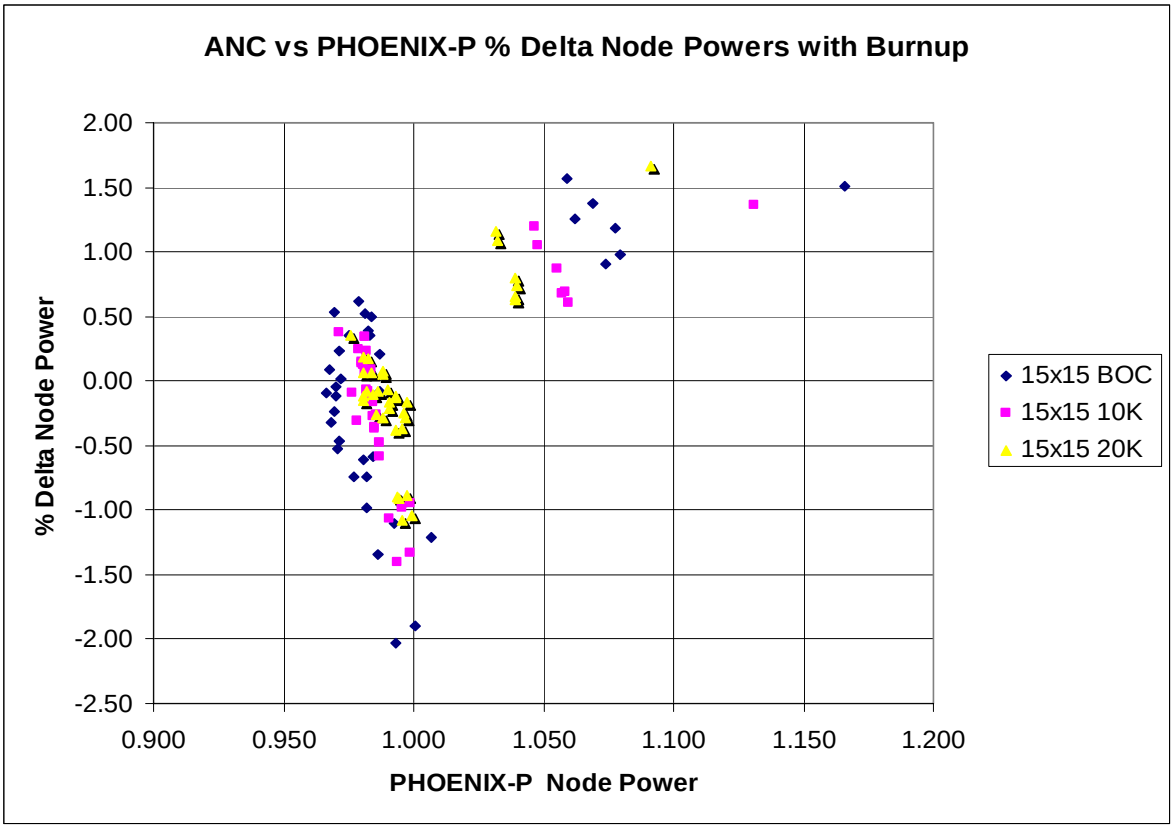

Figure 12
3x3 Model with Large Plausible Gaps - Node Power Accuracy

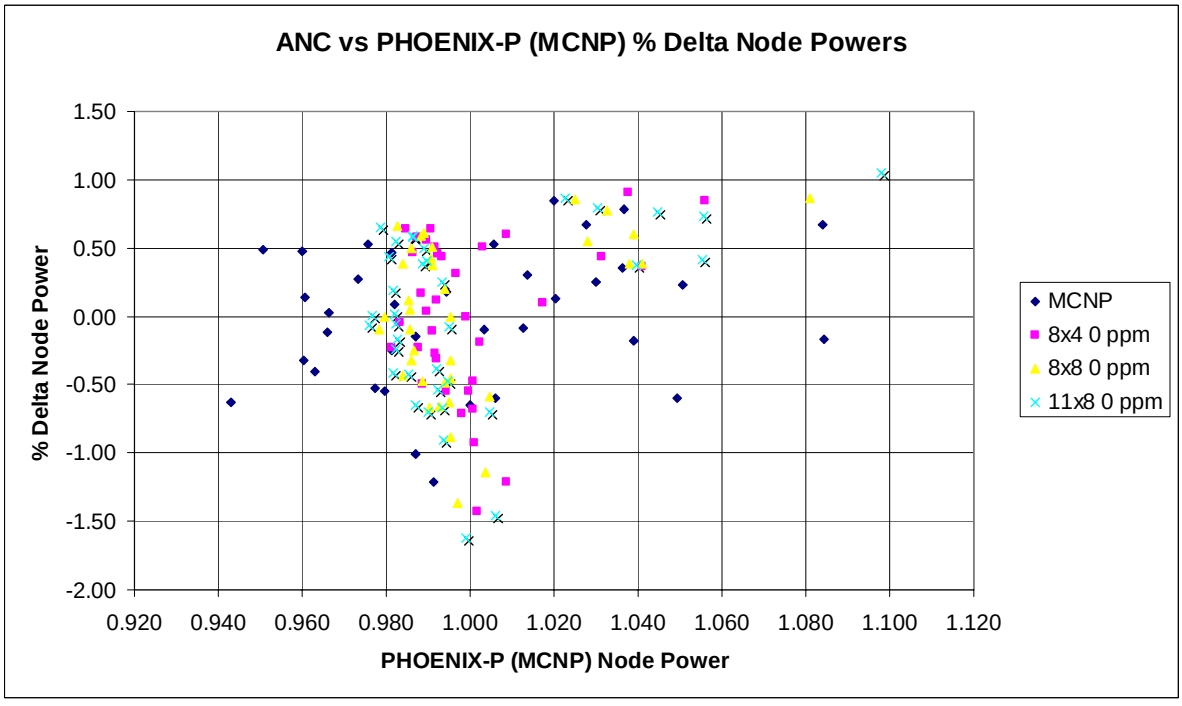

Figure 13
3x3 MCNP Model - Pin Power Accuracy

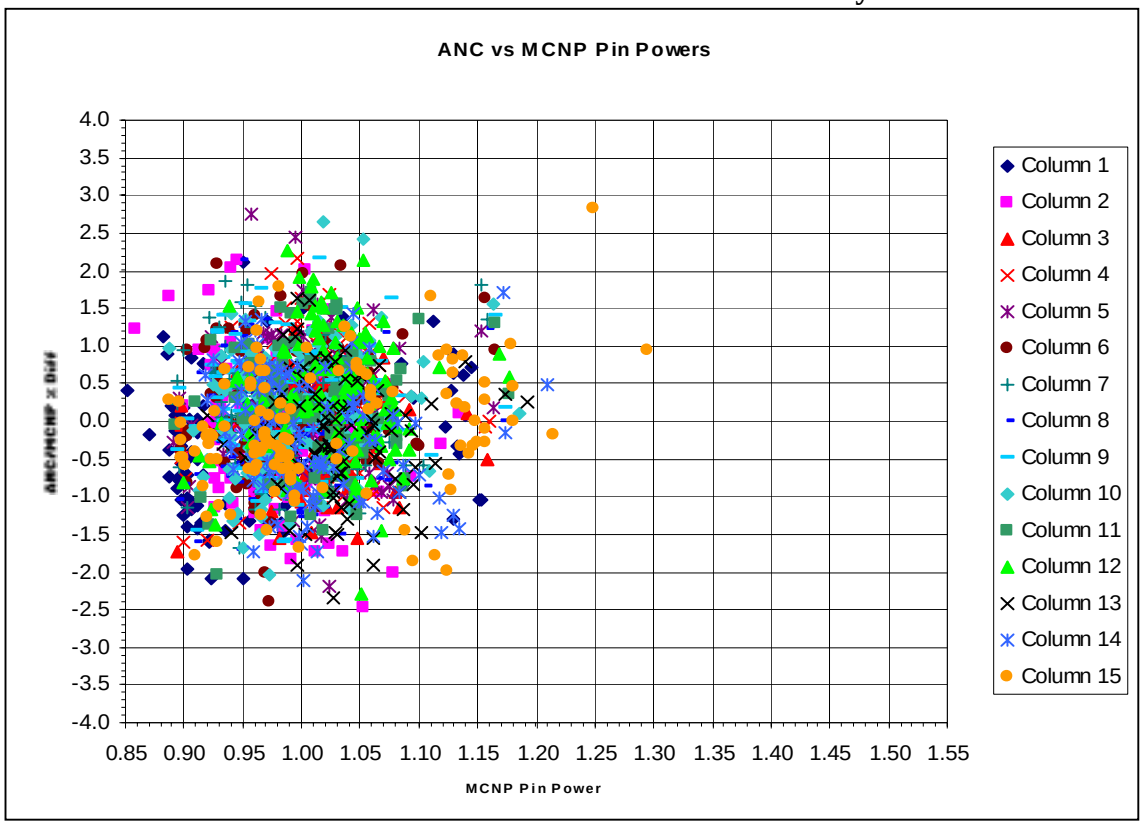

Figure 14
3x3 15.5 mm Gap Model @ 20 GWD/MTU- Pin Power Accuracy